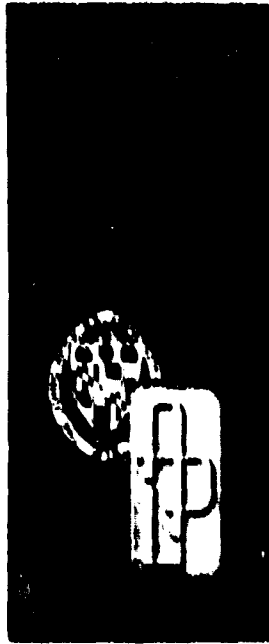


TG-985  
MARCH 1968  
Copy No.

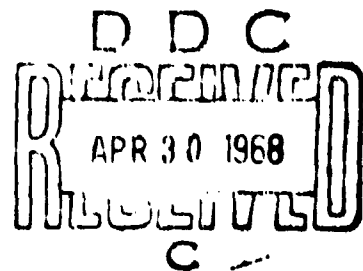


AD 668142

*Technical Memorandum*

**COMPOUND-OGIVE RADOMES  
AS SUBSTITUTE STRUCTURES  
FOR VON KARMAN SHAPES**

BY MANFORD B. TATE

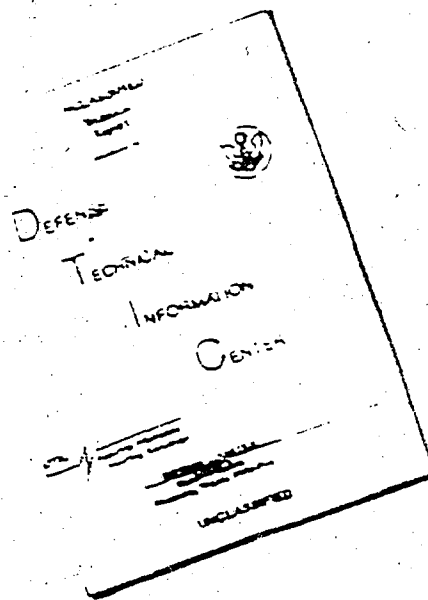


THE JOHNS HOPKINS UNIVERSITY • APPLIED PHYSICS LABORATORY

This document has been approved for public  
release and sale; its distribution is unlimited.

APPLIED PHYSICS LABORATORY

# DISCLAIMER NOTICE



THIS DOCUMENT IS BEST  
QUALITY AVAILABLE. THE COPY  
FURNISHED TO DTIC CONTAINED  
A SIGNIFICANT NUMBER OF  
PAGES WHICH DO NOT  
REPRODUCE LEGIBLY.

THIS DOCUMENT CONTAINED  
BLANK PAGES THAT HAVE  
BEEN DELETED

REPRODUCED FROM  
BEST AVAILABLE COPY

TG-985  
MARCH 1968

*Technical Memorandum*

**COMPOUND-OGIVE RADOMES  
AS SUBSTITUTE STRUCTURES  
FOR VON KARMAN SHAPES**

BY MANFORD B. TATE

THE JOHNS HOPKINS UNIVERSITY • APPLIED PHYSICS LABORATORY  
8621 Georgia Avenue, Silver Spring, Maryland 20910  
Operating under Contract N0w 62-0604-c with the Department of the Navy

This document has been approved for public  
release and sale; its distribution is unlimited

ABSTRACT

A tangent-ogive and three compound-ogive radomes are examined for use of one of them as a substitute structure in analysis of Von Karman radome thermal stresses. A tricentric ogive-cone radome is chosen as the substitute, because it provides a highly satisfactory representation of the Von Karman profile both in regard to approximate duplication of cross-sectional radii ( $r$ ) and coordinate angles ( $\psi$ ) for nearly all values of the spanwise variable ( $x$ ). The introduction of a substitute structure is made necessary by the absence of stress solutions for the Von Karman profile type of structure in current and past technical literature, but a theoretical solution for ogive shapes is available.

Also, the temperature distribution obtained in previous investigations on the Von Karman test radome is herein successfully imposed on the substitute structure with results that agree within two percent of those computed from formulas that were obtained in the earlier studies.

TABLE OF CONTENTS

INTRODUCTION . . . . .	1
NOMENCLATURE . . . . .	2
TRICENTRIC OGIVE-CONE SUBSTITUTE RADOME . . . . .	2
TEMPERATURE DISTRIBUTION . . . . .	7
OTHER SUBSTITUTE STRUCTURES . . . . .	10
SUMMARY . . . . .	17
CONCLUSIONS . . . . .	18
REFERENCES . . . . .	19

LIST OF FIGURES

<u>Figure</u>		<u>Page</u>
1	Tricentric Ogive Cone Radome Compared to Von Karman Shape . . . . .	3
2	Temperature Distribution for Substitute Radome . . . . .	8
3	Multicentric Ogives . . . . .	11
4	Tricentric Ogive Radome Dimensions . . . . .	16

PRECEDING  
PAGE BLANK

LIST OF TABLES

<u>Table</u>		<u>Page</u>
1	Tricentric Ogive-Cone Radome Coordinates .	5
2	Coordinate Comparison for Von Karman and Substitute Radomes . . . . .	6
3	Comparison of Multicentered Ogives with the 28.3" x 6.75" Von Karman Shape . . . . .	13

PRECEDING  
PAGE BLANK

## INTRODUCTION

As a part of the present investigation of radome thermal stresses, a requirement was established to analyze the Von Karman radome that was subjected to aerodynamic heating in OAB\* wind tunnel tests. Owing to the absence of thermal-stress (or any other kind of stress) solutions for the Von Karman profile type of structure in the current and past technical literature and the availability of a theoretical solution for ogive shapes, the writer elected to introduce a substitute structure that was composed of one or more ogives in acceptable representation of the Von Karman test radome. The examination of a tangent-ogive and three compound-ogive profiles is described in this report, and the selection of a substitute radome is made and discussed.

Temperature-distribution functions are derived and explained in References (a) and (b). They furnish the means for specifying and deriving the necessary relations that enable us to impose the Von Karman radome temperatures on the substitute structure, which also is carried out in this report.

The fundamental theory for ogival radomes is derived in Reference (c). Also, since the test radome was constructed of Pyroceram 9606 material, which has heat-variant properties, these properties were put into functional forms in Reference (d).

The highly successful correlations and functional descriptions of the analytical and experimental temperatures that were developed in Reference (a) could not have been obtained without the basic information supplied in References (b) and (e). Reference (b) dealt with the problem of flow conditions around the nose of a blunt radome and provides the general formulas that have made it possible to develop spanwise distribution functions for radome temperatures. In Reference (e), equations are given for the Von Karman radome radii of curvature and the coordinate angle ( $\psi$ ), which has proved to be the essential variable in correlation and mathematical description of the spanwise temperature distributions.

---

\* Ordnance Aerophysics Laboratory, Daingerfield Division, General Dynamics/Pomona.

NOMENCLATURE

A,B:	Constants
F:	Fahrenheit
H:	Intercept parallel to r-axis, inches
K:	Constant
L:	Intercept parallel to z-axis, inches
R:	Radius, inches
T:	Temperature, °F
Z:	Geometric axis of radome
c:	Half-thickness of radome shell wall ( $c = h/2$ ), inches
f:	Function
h:	Wall thickness of radome shell inches
l:	Length, inches
r:	Radius, inches
x:	Wall thickness variable ratio, $x = y/c$
y:	Wall thickness variable, inches
z:	Coordinate along z-axis, inches
ψ:	Coordinate angle, degrees or radians

The following notations are used as subscripts:

a:	Values at outer surface "a"
b:	Values at base of radome
c:	Values at central surface "c"
i,j:	Position indices
o:	Origin or initial (zero)
s:	Values at inner surface "s"

TRICENTRIC OGIVE-CONE SUBSTITUTE RADOME

Coordinates of the Von Karman radome that was used in the OAL wind-tunnel tests are tabulated in References (a) and (e). To represent them, several substitute structures were examined, and it was found that the compound form shown in Figure 1 provides satisfactory agreement with the Von Karman profile, which was drawn also on Figure 1 for comparison with the substitute structure. Other proposed substitutes were reviewed and are discussed subsequently.

The compound ogive pictured in Figure 1 describes the exterior surface of a radome whose profile is composed of four parts. Starting at the base, a 3.34-caliber tangent ogive extends along the length for nine inches ( $0 \leq z \leq 9$ ). A conical segment is employed over the next nine inches ( $9 \leq z \leq 18$ ). The third

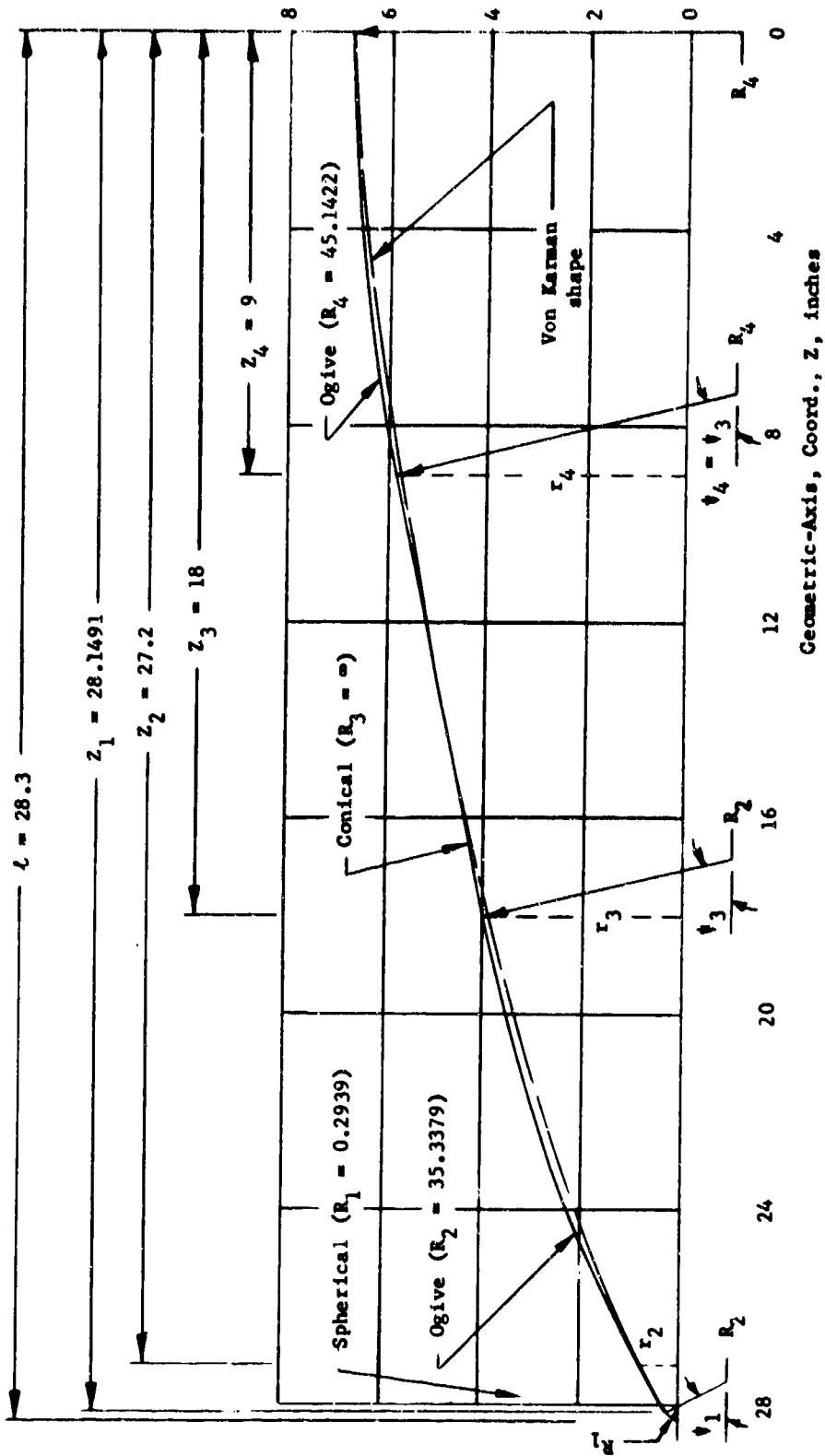


Fig. 1 Tricentric Ogive Cone Radome Compared to Von Karman Shape

part is a 4.40-caliber secant ogive that lies between  $x = 18$  inches and approximately 28.15 inches. The final part is a spherical segment serving as a nose to complete the radome length to 28.3 inches.

The coordinates of the foregoing tricentric ogive-cone profile are given in general for the ogival segments by

$$r = R_1 \sin \psi - H_1, \quad z = R_1 \cos \psi + L_1 \quad (1)$$

where  $H_1$  and  $L_1$  are intercept heights and lengths that respectively parallel the  $r$  and  $z$  coordinate axes. And the conical-section coordinate  $r$  is expressed in terms of coordinate  $z$ ; e.g.,

$$r = r_1 + (z_1 - z) \cot \psi_1 \quad (2)$$

where  $r_1$  and  $z_1$  may be the coordinates at either end of the conical segment, and  $\psi_1$  is constant (in Figure 1,  $\psi_1 = \psi_3 = \psi_4 = 78^\circ 30'$ ). Specifically, in relation to the substitute structure of Figure 1, we have

$$r = 0.2939 \sin \psi, \quad z = 0.2929 \cos \psi + 28.0061,$$

$$0 \leq \psi \leq 60^\circ 53' 04'', \quad (29.3 \geq z \geq 28.1491) \quad (3)$$

$$r = 35.3379 \sin \psi - 30.6158, \quad z = 35.3379 \cos \psi + 10.9547$$

$$60^\circ 53' 04'' \leq \psi \leq 78^\circ 30', \quad (28.1491 \geq z \geq 18) \quad (4)$$

$$r = 4.0124 + 0.20345(18 - z), \quad 18 \geq z \geq 9, \quad (\psi = 78^\circ 30') \quad (5)$$

$$r = 45.1422 \sin \psi - 38.3922, \quad z = 45.1422 \cos \psi, \quad 78^\circ 30' \leq \psi \leq 90^\circ,$$

$$(9 \geq z \geq 0) \quad (6)$$

TABLE 1. Tricentric Ogive-Cone Radome Coordinates

x (in.)	r (in.)	R (in.)	H (in.)	L (in.)	$\psi$ (deg-min-sec)	sin $\psi$	cos $\psi$
28.3	0	0.2939	0	28.0061	0	0	1
28.24	0.1769	"	"	"	37-00-25	0.601,915	0.798,566
28.1491	.2568	"	"	"	60-53-04	.873,640	.486,572
27.9	.3942	35.3379	30.6158	10.9547	61-20-45	.877,528	.479,522
27.3	.7147	"	"	"	62-26-55	.886,598	.462,543
27.2	.7664	"	"	"	62-37-52	.888,063	.459,714
26.3	1.2163	"	"	"	64-15-46	.900,791	.434,245
25.3	1.6794	"	"	"	66-02-58	.913,897	.405,947
24.3	2.1054	"	"	"	67-48-44	.925,951	.377,648
23.3	2.4956	"	"	"	69-33-09	.936,995	.349,350
21.225	3.1966	"	"	"	73-06-15	.956,832	.290,631
19.5	3.6735	"	"	"	76-00-22	.970,326	.241,817
18	4.0124	"	"	"	78-30-00	.979,920	.199,370
14.15	4.7957	"	"	--	"	"	"
11.9365	5.2461	"	"	--	"	"	"
9	5.8435	"	"	--	"	"	"
7.075	6.1920	45.1422	38.3922	0	80-58-59	.987,639	.156,727
4.3	6.5433	"	"	"	84-31-03	.995,422	.095,255
0	6.75	"	"	"	90	1	0

and values calculated from these coordinate relations are listed in Table 1 for employment in the subsequently discussed temperature-distribution computations and in Table 2 for comparison with the Von Karman radome coordinates.

TABLE 2. Coordinate Comparison For Von Karman and Substitute Radomes

z (in)	$\psi$ , Von Karman (deg-min-sec)	$\psi$ , Fig. 1 Sub. (deg-min-sec)	r, Von Karman (in)	r, Fig. 1 Sub. (in)	r-Diff. (%)
28.3	0	0	0	0	0
27.3	62-02	62-26-55	0.7128	0.7147	0.27
27.2	62-37-52	62-37-53	0.7654	0.7664	0.13
26.3	66-13	64-15-46	1.1924	1.2163	2.00
25.3	68-34	66-02-58	1.6072	1.6794	4.49
24.3	70-12	67-48-44	1.9828	2.1054	6.18
23.3	71-27	69-33-09	2.3304	2.4956	7.09
21.225	73-26-14	73-06-15	2.9845	3.1966	7.11
19.5	74-43-51	76-00-22	3.4758	3.6735	5.69
18	75-42-27	78-30	3.8714	4.0124	3.64
14.15	77-52-50	"	4.7730	4.7957	0.48
11.9365	79-03-45	"	5.2345	5.2461	0.22
9	80-34-44	"	5.7533	5.8435	1.57
7.075	81-39-34	80-58-59	6.0543	6.1920	2.27
4.3	83-27-35	84-31-03	6.4184	6.5433	1.95
0	90	90	6.75	6.75	0

From the preceding Table 2, we see that at equal z-distances the computed percentage r-differences increase to slightly more than seven percent and then varyingly decrease to zero at the radome bases. Inasmuch as all the r-values of the substitute structure are larger than the original radii, the substitute is slightly roomier than the 28.3" x 6.75" Von Karman radome.

### TEMPERATURE DISTRIBUTION

As a rule, the temperature distribution in an ogival radome cannot be described by the same functions of the coordinate angle ( $\psi$ ) as those obtained for a Von Karman radome, even when the outer-surface profiles substantially coincide as depicted in Figure 1. The Von Karman radome temperature distribution can, however, be imposed on the ogive structure by successive functions restricted to specified intervals along the length of the substitute structure. This procedure was followed in the present instance with the results shown in Figure 2.

It was demonstrated in Reference (a) that the Von Karman radome's outer surface temperature distribution ( $T_a$ ) can be represented by general formulas developed in Reference (b) by inserting empirical coefficients. From equation (1) of Reference (a), the general relation in the transonic zone is

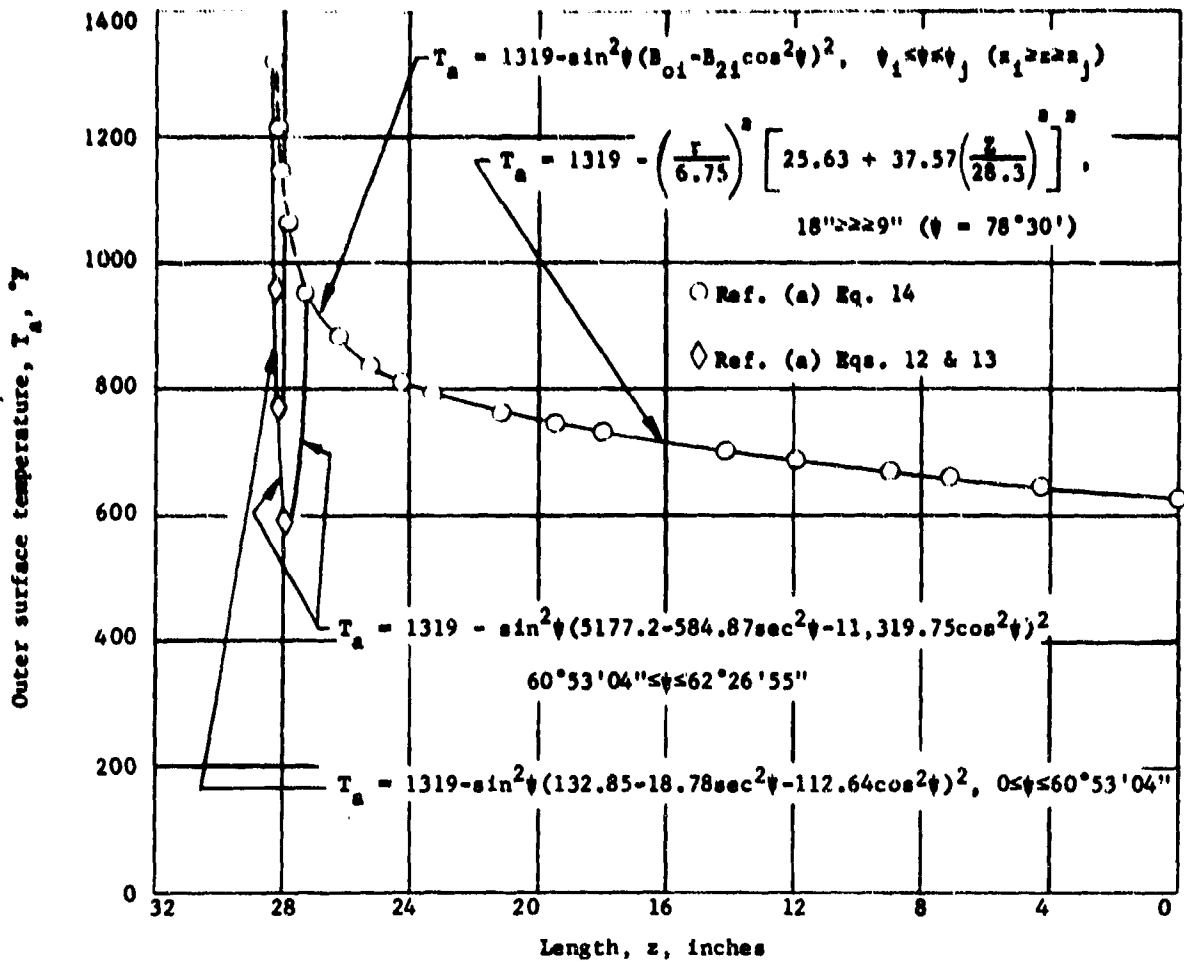
$$T_a = T_{a0} - \sin^2 \psi (A_0 + A_1 \sec^2 \psi - A_2 \cos^2 \psi)^2 \quad (7)$$

where the  $A_i$  are empirically determined, and  $T_{a0} = (T_a)_{\psi=0}$  is the temperature at the tip, or leading edge, of the radome. The interval over which the equation is applicable can be found from test data, or it can be calculated by analyses of heat exchange from air to radome with conduction in the wall toward the radome's base. The latter method was used to secure the reference data reported in Figure 4 of Reference (a). These temperature data were computed for the transference of heat through the boundary layer starting with laminar flow followed by a transition to turbulent flow based on a specified Reynold's number. The Taylor-McColl conical-flow theory and heat-transfer analyses were used as explained in Reference (f) on the computer program.

Beyond the transonic zone, the general formula is

$$T_a = T_{a0} - \sin^2 \psi (B_0 - B_2 \cos^2 \psi)^2 \quad (8)$$

where again the  $B_i$  are empirically determined.



$\psi_i$ (deg-min-sec)	$\psi_j$ (deg-min-sec)	$z_i$ (in.)	$z_j$ (in.)	$B_{0i}$	$B_{zi}$	Eq. No.
0	60-53-04	28.3	28.15	14.88	-3.61	11
60-53-04	62-26-55	28.15	27.3	84.49	293.66	12
62-26-55	66-02-58	27.3	25.3	32.68	51.48	13
66-02-58	78-30	25.3	18	24.95	4.56	14
78-30	90	9	0	26.13	3.35	16

Fig. 2 Temperature Distribution for Substitute Radome

By means of the regression formulas developed in Reference (a), the following equations were obtained to impose the Von Karman test radome temperature distribution on the exterior surface shown in Figure 1 for the substitute radome.

$$T_a = 1319 - \sin^2 \psi (132.85 - 18.78 \sec^2 \psi - 112.64 \cos^2 \psi)^2, \quad 0 \leq \psi \leq 60^\circ 53' 04'' \quad (9)$$

$$T_a = 1319 - \sin^2 \psi (5177.20 - 584.87 \sec^2 \psi - 11,319.75 \cos^2 \psi)^2$$

$$60^\circ 53' 04'' \leq \psi \leq 62^\circ 26' 55'' \quad (10)$$

For the dashed curves at the top of Figure 2,

$$T_a = 1319 - \sin^2 \psi (14.88 + 3.61 \cos^2 \psi)^2, \quad 0 \leq \psi \leq 60^\circ 53' 04'' \quad (11)$$

$$T_a = 1319 - \sin^2 \psi (84.99 - 293.66 \cos^2 \psi)^2, \quad 60^\circ 53' 04'' \leq \psi \leq 62^\circ 26' 55'' \quad (12)$$

and for the solid curves beyond the transonic zone in Figure 2,

$$T_a = 1319 - \sin^2 \psi (32.68 - 51.48 \cos^2 \psi)^2, \quad 62^\circ 26' 55'' \leq \psi \leq 66^\circ 02' 58'' \quad (13)$$

$$T_a = 1319 - \sin^2 \psi (24.95 - 4.56 \cos^2 \psi)^2, \quad 62^\circ 02' 58'' \leq \psi \leq 78^\circ 30' \quad (14)$$

$$T_a = 1319 - (r/6.75)^2 [25.63 + 37.57(z/28.3)^2]^2, \quad 18'' \leq z \leq 9'', (\psi = 78^\circ 30') \quad (15)$$

$$T_a = 1319 - \sin^2 \psi (26.13 - 3.35 \cos^2 \psi)^2, \quad 78^\circ 30' \leq \psi \leq 90^\circ \quad (16)$$

where equations (9) to (14) and (16) apply along the curved portions of the substitute radome, and equation (15) holds in the conical section. Equation (15) is expressed in terms of the coordinate variables (r, z) of the cone in the form

$$T_a = T_{a0} - (r/r_b)^2 [ B_0 - B_2 (z/l)^2 ]^2 \quad (17)$$

because  $\psi = 78^\circ 30'$  is constant for the cone, but  $r/r_b$  and  $z/l$  furnish variations that are analogous to the sine and cosine effects in the other equations. And the dashed-curve equations (11) and (12) were obtained in order to study their influence on the thermal stresses when they are used instead of equations (9) and (10).

The preceding relationships lead to values that agree within two percent of the plotted temperatures for the Von Karman radome (Figure 2); and when we employ  $f(x)$  shown below for the wall-thickness temperature distribution, we find that the temperatures inside the radome wall and along its inner and outer surfaces can be computed from

$$T = T_a f(x) \quad (18)$$

where  $T = T(\psi, x)$  is the temperature at any point in or on the wall,  $T_a = T_a(\psi)$  is given by equations (9) and (10), or (11) and (12), and (13) to (16), inclusive, and  $f(x) = f(y/c)$  is

$$f(x) = 0.257 + 0.358x + 0.305x^2 + 0.084x^3 \quad (19)$$

which was derived in Reference (a) for the Von Karman test radome.

Therefore, by means of the foregoing expressions, one can reproduce the temperature distribution in the substitute structure that was found for the Von Karman radome in Reference (a).

#### OTHER SUBSTITUTE STRUCTURES

The other structures that were examined as potential substitutes for the 28.3" x 6.75" Von Karman radome are shown in Figures 3 and 4.

The tangent ogive (Figure 3-a) that has the same length (28.3") and base radius (6.75") as the Von Karman radome is a 4.64-caliber ogive. Its

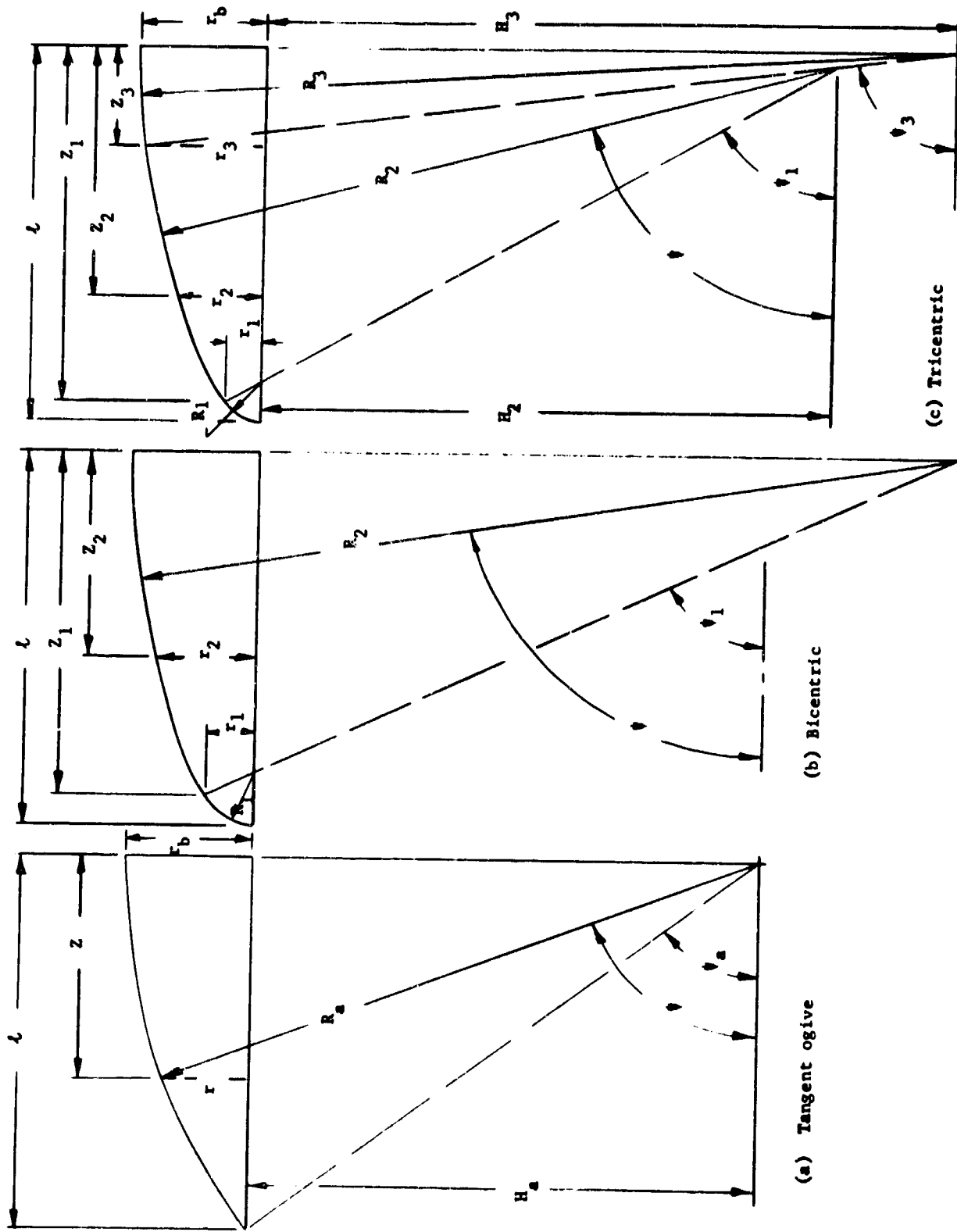


Fig. 3 Multicentric Ogives

dimensions can be calculated from the following expressions:

$$R_a = \frac{r_b}{2} + \frac{l^2}{2r_b} = 62.7002'' \quad (20)$$

$$H_a = R_a - r_b = 55.9502'' \quad (21)$$

$$\sin \psi_a = \frac{H_a}{R_a} = 0.892,345; \quad \cos \psi_a = \frac{l}{R_a} = 0.451,354; \quad \psi_a = 63^\circ 10' 09'' \quad (22)$$

and its  $r$  and  $z$  coordinates are given by

$$r = R_a \sin \psi - H_a = R_a (\sin \psi - \sin \psi_a), \quad z = R_a \cos \psi \quad (23)$$

but one observes immediately that this radome has a sharp point with an angular value ( $\psi_a$ ) at the tip, whereas the original radome is blunt nosed with  $\psi = 0$  at the tip. A further comparison is made in Table 3 with  $r$ -radii computed at the quarter points of the span and at one inch from the tip. It is seen in the Table 3 results that the  $r$ -discrepancies vary from -30.6 percent at one inch from the tip to +7.5 percent at the mid-point of the span, with the first percentage being too much for acceptance.

The bicentric ogive of Figure 3-b constitutes a first step toward improvement over the tangent ogive for simulation of the Von Karman shape. Only one set of coordinates can be prescribed by requiring them to equal the corresponding Von Karman profile coordinates. If we choose  $r_2, z_2$  in Figure 3-b, the ogive radii and other dimensions are determined by

$$R_2 = \frac{r_b - r_2}{2} + \frac{z_2^2}{2(r_b - r_2)}, \quad H_2 = R_2 - r_b \quad (24)$$

$$R_1 = \frac{R_2 + l}{2} - \frac{H_2^2}{2(R_2 - l)}, \quad L_1 = l - R_1 \quad (25)$$

TABLE 3. Comparison of Multicentered Ogives with the 28.3" x 6.75" Von Karman Shape.

z (in)	Von Karman		Tangent Ogive (Fig. 3-a)		Bicentric Ogive (Fig. 3-b)		Tricentric Ogive (Fig. 3-c & 4)		
	↓ (d-m-s)	r (in)	↓ (d-m-s)	r (in)	↓ (d-m-s)	r (in)	↓ (d-m-s)	r (in)	r-Diff (%)
28.3	0	0	63-10-09	0	0	0	0	0	0
27.3	62-02	0.7128	64-11-20	0.4947	65-05-07	0.7190	62-37-52	0.7266	-5.1
27.2	62-37-52	0.7654	70-12-48	3.0374	65-10-57	0.7654	69-56-54	3.3507	+12.3
21.225	73-26-14	2.9845	76-57-26	5.1324	70-52-52	3.1753	78-12	5.3699	+12.5
14.15	77-52-50	4.7730	83-31-15	6.3493	77-23-16	5.1862	84-31	6.4109	+5.9
7.075	81-39-34	6.0543	90	6.75	83-43-57	6.3623	90	6.75	0
0	90	6.75							

$$\sin \psi_1 = \frac{H_2}{R_2 - R_1}, \quad \cos \psi_1 = \frac{L_1}{R_2 - R_1} \quad (26)$$

$$r_1 = R_1 \sin \psi_1 = R_2 \sin \psi_1 - H_2, \quad z_1 = R_1 \cos \psi_1 + L_1 = R_2 \cos \psi_1 \quad (27)$$

and, if we choose  $z_2 = 27.2''$  and  $r_2 = 0.7654''$  as in Tables 2 and 3 for the Von Karman shape, we find

$$\begin{array}{ll} R_2 = 64.804'' & \sin \psi_1 = 0.901,250 \\ H_2 = 58.054 & \cos \psi_1 = 0.433,299 \\ L_1 = 27.911 & \psi_1 = 64^\circ 19' 23'' \\ R_1 = 0.389 & z_1 = 28.0795'' \\ H_1 = L_2 = 0 & r_1 = 0.3506 \end{array} \quad (28)$$

with which the coordinates can be calculated from equations (1).

Further comparison between this bicentric ogive and the Von Karman form is given in Table 3 where the cross-sectional radii appear to agree fairly well; but the surface slopes (measured by  $\psi$ ) were found to be unsatisfactory, especially at about one inch from the tip ( $z = 27.2''$  and  $27.3''$  in Table 3).

In an effort to improve the angular correspondence, the tricentric ogive shown in Figures 3-c and 4 was examined. When two sets of coordinates are prescribed, say  $(r_2, z_2)$  and  $(r_3, z_3)$  in Figure 3-c, the ogive radii ( $R_1$ ), the intercepts ( $H_1$  and  $L_1$ ), and the angles ( $\psi_1$ ) can be calculated with the following group of equations.

$$R_3 = \frac{r_b - r_3}{2} + \frac{z_3^2}{2(r_b - r_3)}, \quad H_3 = R_3 - r_b \quad (29)$$

$$\sin \psi_3 = \frac{r_3 + H_3}{R_3}, \quad \cos \psi_3 = \frac{z_3}{R_3}, \quad K = \frac{r_3 - r_2}{z_2 - z_3} \quad (30)$$

$$\sin \psi_2 = \frac{(1-K^2) \sin \psi_3 + 2K \cos \psi_3}{(1+K^2)}, \quad \cos \psi_2 = \frac{2K \sin \psi_3 + (K^2-1) \cos \psi_3}{(1+K^2)} \quad (31)$$

$$R_2 = \frac{r_3 - r_2}{\sin \psi_3 - \sin \psi_2} = \frac{z_2 - z_3}{\cos \psi_2 - \cos \psi_3} \quad (32)$$

$$H_2 = H_3 + (R_2 - R_3) \sin \psi_3, \quad L_2 = (R_3 - R_2) \cos \psi_3 \quad (33)$$

$$R_1 = \frac{R_2 + l - L_2}{2} - \frac{H_2^2}{2(R_2 - l + L_2)}, \quad L_1 = l - R_1 \quad (34)$$

$$\sin \psi_1 = \frac{H_2}{R_2 - R_1}, \quad \cos \psi_1 = \frac{L_1 - L_2}{R_2 - R_1} \quad (35)$$

$$r_1 = R_1 \sin \psi_1, \quad z_1 = R_1 \cos \psi_1 + L_1 \quad (36)$$

The following dimensions were calculated with the foregoing expressions for the tricentric ogive drawn on Figure 4.

$z_1 = 28.1767''$	$z_2 = 27.2''$	$z_3 = 11.9365''$	
$r_1 = 0.2078$	$r_2 = 0.7266$	$r_3 = 5.7815$	
$H_1 = 0$	$H_2 = 44.6836$	$H_3 = 67.2913$	
$L_1 = 28.0633$	$L_2 = 3.6930$	$L_3 = 0$	(37)
$R_1 = 0.2367$	$R_2 = 51.1340$	$R_3 = 74.0413$	
$\psi_1 = 61^\circ 23' 32''$	$\psi_2 = 62^\circ 37' 52''$	$\psi_3 = 80^\circ 43' 22''$	
$\sin \psi_1 = 0.877,917$	$\sin \psi_2 = 0.888,063$	$\sin \psi_3 = 0.986,919$	
$\cos \psi_1 = 0.478,814$	$\cos \psi_2 = 0.459,714$	$\cos \psi_3 = 0.161,214$	

It may be noted from Table 3 that the tricentric ogive of Figure 4 is unsuitable owing to radial deviations of approximately 12.5 percent along the span between the three-quarter point and the midpoint.

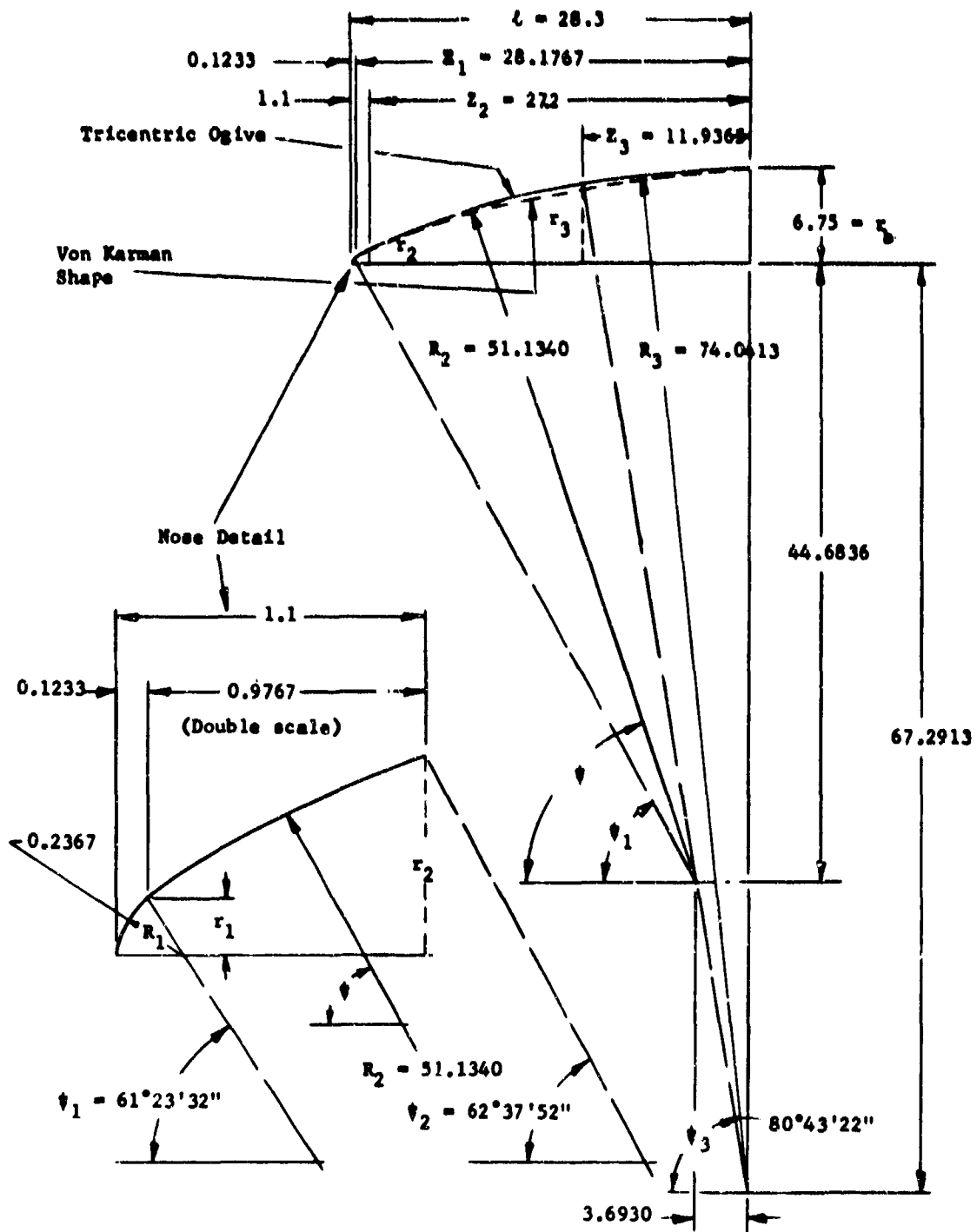


Fig. 4 Tricentric-Ogive Radome Dimensions

A few other arrangements were examined in the manner described in the preceding paragraphs, and it was concluded that the compound ogive of Figure 1 optimized the desirable features discussed in this section.

#### SUMMARY

A tangent ogive and three compound-ogive radomes were compared with the 28.3" x 6.75" Von Karman radome to select a substitute structure for the analysis of thermal stresses. The Von Karman radome was used in the OAL aerodynamic heating tests in which inner wall temperatures and thermal strains were measured at a few points for verification of temperature and stress computations. The compound ogive shown in Figure 1 was selected as a good substitute for the Von Karman shape.

After selection of a suitable substitute, the Von Karman test-radome temperature distribution that was obtained in earlier investigations (References (a) and (b)) was imposed on the substitute radome. This was done on a piecewise basis along the span because one-to-one correspondence between the Von Karman shape and any other profile is unobtainable with a single function. On the substitute radome, six functions were employed to impose the temperatures that are described by three functions for the Von Karman radome. The resulting expressions give the desired temperatures within computed percentages of plus or minus two percent.

The approach that is summarized in the two preceding paragraphs was adopted owing to the absence of thermal-stress solutions for the Von Karman profile type of structure in current and past technical literature and the availability of a theoretical solution for the ogive forms.

CONCLUSIONS

Based on the present studies and the referenced information, it is concluded that:

(1) The tricentric ogive-cone radome selected herein provides a fully satisfactory substitute for the 28.3" x 6.75" Von Karman radome in regard to the evaluation of thermal stresses.

(2) The temperature functions developed herein furnish good duplication of the distribution in the Von Karman test radome, coming within two percent of the values computed from equations that were evolved in a previous investigation.

REFERENCES

- (a) Tate, M. B. "Statistical Analysis of Temperature Data from Wind Tunnel Test of a Von Karman Radome," (Confidential) APL/JHU TG-983, 1968.
- (b) Tate, M. B. "Air Properties and Flow Conditions Around the Nose of a Blunt Radome," (Unclassified) APL/JHU TG-981, 1968.
- (c) Tate, M. B. "Large Axisymmetric Thermal Bending Stresses in Ogival Radomes with Heat Variant Material Properties," (Unclassified) APL/BBE EM-3995, 1965.
- (d) Tate, M. B. "Functionalization of Pyroceram 9606 Test Data for Radome Thermal-Stress Analysis," (Unclassified) APL/JHU TG-980, 1968.
- (e) Tate, M. B. "Curvature Radii and Derivatives for Thermal-Stress Analysis of Von Karman Radomes," (Confidential) APL/JHU TG-982, 1968.
- (f) Suess, R. P. "IBM 8094 Computer Program for the Computation of Radome Thermal Stresses," (Unclassified) APL/BBE EM-3854, 1964.

UNCLASSIFIED

Security Classification

DOCUMENT CONTROL DATA - R & D		
<i>Security classification of title, body of abstract and indexing annotation must be entered when the overall report is classified</i>		
1. ORIGINATING ACTIVITY (Corporate author) The Johns Hopkins University, Applied Physics Lab. 8621 Georgia Ave., Silver Spring, Maryland		2a. REPORT SECURITY CLASSIFICATION Unclassified
		2b. GROUP n. a.
3. REPORT TITLE  Compound-Ogive Radomes as Substitute Structures for Von Karman Shapes		
4. DESCRIPTIVE NOTES (Type of report and inclusive dates) Technical Memorandum		
5. AUTHOR(S) (First name, middle initial, last name)  Manford B. Tate		
6. REPORT DATE March 1968	7a. TOTAL NO. OF PAGES 19	7b. NO. OF REFS 6
8a. CONTRACT OR GRANT NO. NOW 62-0604-c	8b. ORIGINATOR'S REPORT NUMBER(S)  TG-985	
b. PROJECT NO.  c.  d.	9b. OTHER REPORT NO(S) (Any other numbers that may be assigned this report)	
10. DISTRIBUTION STATEMENT  This document has been approved for public release and sale; its distribution is unlimited.		
11. SUPPLEMENTARY NOTES		12. SPONSORING MILITARY ACTIVITY  Naval Ordnance Systems Command
13. ABSTRACT <p>A tangent-ogive and three compound-ogive radomes are examined for use of one of them as a substitute structure in analysis of Von Karman radome thermal stresses. A tricentric ogive-cone radome is chosen as the substitute, because it provides a highly satisfactory representation of the Von Karman profile both in regard to approximate duplication of cross-sectional radii (<math>r</math>) and coordinate angles (<math>\theta</math>) for nearly all values of the spanwise variable (<math>z</math>). The introduction of a substitute structure is made necessary by the absence of stress solutions for the Von Karman profile type of structure in current and past technical literature, but a theoretical solution for ogive shapes is available.</p> <p>Also, the temperature distribution obtained in previous investigations on the Von Karman test radome is herein successfully imposed on the substitute structure with results that agree within two percent of those computed from formulas that were obtained in the earlier studies.</p>		

DD FORM 1 NOV 65 1473

UNCLASSIFIED  
Security Classification

UNCLASSIFIED

Security Classification

14.

KEY WORDS

Compound-ogive radomes  
Substitute radome structures  
Radome configurations  
Von Karman shape

UNCLASSIFIED

Security Classification